[5] A. Leupp and M. J. O. Strutt, "Noise behaviour of the MOSFET at VHF and UHF," *Electron. Lett.*, vol. 4, no. 15, July 1968.
[6] ——, "High-frequency FET noise parameters and approximation of the optimum source admittance," *IEEE Trans. Electron Devices*, vol. ED-16, pp. 428–431, May 1969.

State-Space Analysis of a Magnetically Tuned IMPATT Oscillator Lumped Model

I. J. H. S. MOORE AND J. A. C. STEWART

I. Introduction

One method of frequency modulating an IMPATT-diode oscillator uses a ferrite whose susceptibility is a function of applied dc magnetic field. Octave band tuning of Gunn oscillators using yttrium iron garnet (YIG) has been reported by several authors [1], [2]. The YIG comprised the principal energy-storage element apart from the active device. For applications requiring relatively small frequency deviations (500 MHz), a YIG sphere can be used to perturb the resonant frequency of the oscillator cavity, and hence to vary the oscillation frequency. This short paper describes the derivation and analysis of a lumped model of the YIG tuned cavity IMPATT oscillator.

While a large-signal time-domain solution of the equations resulting from the lumped model has been obtained, the computer time required for a steady-state solution is prohibitive. In addition, the complex microwave circuit can support frequencies which are not harmonically related, which makes it difficult to interpret the large-signal waveforms in terms of frequency components. By using the small-signal form of the diode lumped model equations, the complex natural frequencies for the complete system can be evaluated for given values of dc magnetic field [3]. Comparison of computed and experimental oscillator tuning results indicates that the small-signal IMPATT-diode model should be modified to account for large-signal effects. The modified oscillator model shows good agreement with experimental results, and hence may be used as a tool to investigate further the oscillator tuning behavior.

In the analysis, the YIG tuned oscillator is subdivided into three distinct regions: the IMPATT-diode chip, the microwave circuit external to the chip and YIG sphere, and the YIG tuning sphere. By sectioning the oscillator components in this manner, it is possible to use this approach to analyze many differing oscillator configurations. The derivation of lumped models for these separate regions is described in Sections II–IV, respectively. State-space analysis of the complete oscillator lumped model is discussed in Section V. Section VI indicates the large-signal modifications to the small-signal diode lumped model. The validity of the model, in comparison with experimental measurements, is demonstrated in Section VII.

II. IMPATT-Diode Lumped Model

A small-signal lumped model of an IMPATT diode exists, which includes realistic hole and electron ionization rates and saturation velocities [3]. The model is accurate for p-i-n type structures, but becomes less accurate for diodes with more localized avalanche regions. A uniform avalanche region dc electric field is assumed, equal to the maximum dc electric field in the depletion region. The avalanche region width is found using the ionization integral for this p-i-n diode approximation. Fig. 1(b), which indicates the ionization rate for electrons, α_n for a n^+-p-p^+ diode demonstrates the inadequacy of the uniform electric field approximation. In the present model, therefore, the ionization-rate curves are approximated by a series of steps, as shown in the figure.

Solution of the steady-state continuity equations for holes and electrons, and Poisson's equation, yields, for a given bias current, the electric field and hole and electron current profiles in the diode depletion layer [Fig. 1(a)]. In order to speed up the computation, the

Manuscript received August 15, 1972; revised December 8, 1972. This work was supported by the Science Research Council, England.
The authors are with the Department of Electrical and Electronic Engineering, Ashby Institute, Queen's University, Belfast, Northern Ireland.

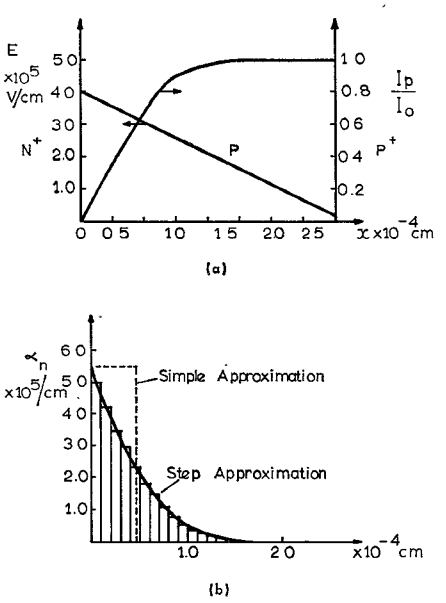

Fig. 1. (a) Static electric field and hole current profiles in n^+-p-p^+ diode depletion layer. (b) Electron ionization rate approximations in n^+-p-p^+ diode depletion layer.

avalanche region width is defined as the distance from the junction at which the hole current reaches 98 percent of its final value. The average dc electric fields in the avalanche lumps are perturbed until the ionization integrals approach unity to within a specified tolerance. The values of α_n and α_p are then computed for each lump and used to evaluate the small-signal diode behavior [3]. Fig. 2 contrasts the diode small-signal impedance at a dc bias current of 20 mA computed 1) using the simple small-signal model, 2) using the modified small-signal model, and 3) using a model which evaluates the large-signal diode impedance as a function of RF applied voltage. The curve is obtained for low values of RF applied voltage. The modified small-signal model is seen to be consistent with the large-signal model over the normal diode operating frequency range, while requiring only a fraction of the computer time. The diode parameters are: cross-sectional area $=0.9\times10^{-4}$ cm^2, depletion layer width $=2.7\times10^{-4}$ cm, epitaxial layer doping density $=0.9\times10^{16}$ cm^{-3}, saturated electron velocity $=8.5\times10^6$ cm$\cdot$s^{-1}, and saturated hole velocity $=7.0\times10^6$ cm$\cdot$s^{-1}.

The state variables used to describe the diode behavior are the small-signal electric fields at the lump edges and the total small-signal hole charges in the lump. The model results in a set of state equations. The variables used to couple the diode to the external circuit are the small-signal diode voltage and current.

III. Microwave External Circuit Model

The external microwave circuit is separated into two regions: a uniform transmission-line region, which in this study may consist of a coaxial-line or a radial-line section, and the diode pill encapsulation and mount.

The uniform line may be described by a ladder network of lumped elements. For a reasonably accurate representation, each section of the ladder network should be equivalent to a line length less than $\lambda/15$, where λ is the operating wavelength. The lumped-element values are determined from the capacitance and inductance per unit length of the transmission line in question. This uniform-line equivalent circuit includes the cavity coupling capacitor and load resistance.

At the microwave frequencies considered in this paper, a simple two-element equivalent circuit for the diode pill encapsulation may be used. Losses in the encapsulation and diode series resistance are included in the resistance R_s. Following Getsinger [4], the diode mount, consisting of the transforming section between the pill outer circumference and the uniform line, may be characterized by lumped elements. A modified form of Getsinger's fringing capacitances is used to more precisely describe the mount.

The lumped-element equivalent circuit for the microwave external circuit consists of a ladder network of series inductances and shunt capacitances. By defining the state variables as the inductor currents

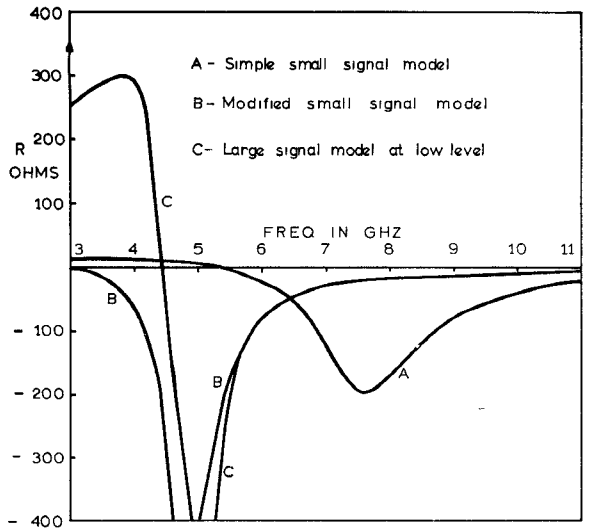

Fig. 2. Diode small-signal impedance at 20.0-mA bias current. (a) Real part of impedance versus frequency. (b) Imaginary part of impedance versus frequency.

and capacitor voltages, a set of state equations describing the circuit behavior results [3].

IV. YIG Sphere State Equations

The YIG sphere, assumed small compared with the operating wavelength, may be represented by a set of state equations [5]. After applying small-signal approximations to the Landau–Lifschitz form of the equation of motion of the sphere magnetization vector, three state equations result relating magnetization vector components m_x, m_y, and m_z and the small-signal magnetic field, assumed uniform and in the x direction h_x:

$$\begin{aligned} \dot{m}_x &= -\alpha\gamma H_0 m_x - \gamma H_0 m_z + \alpha\gamma M_0 h_x \\ \dot{m}_y &= 0 \\ \dot{m}_z &= \gamma H_0 m_x - \alpha\gamma H_0 m_z - \gamma M_0 h_x \end{aligned} \tag{1}$$

where γ is the gyromagnetic ratio, α is the damping factor, M_0 is the saturation magnetization, and H_0 is the dc magnetic field.

The coupling of the sphere to the microwave cavity, and hence to the diode, is calculated using the reciprocity theorem by representing the sphere as a fictitious loop antenna [6], [see Fig. 3(a)]. Equating the magnetic moments of the sphere and the equivalent loop antenna

$$i_x A = m_x V_s \tag{2}$$

where A is the loop area and V_s the sphere volume.

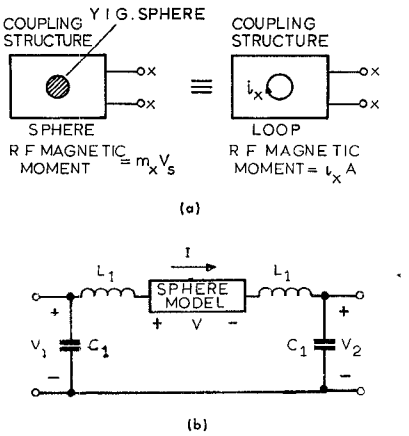

Fig. 3. (a) Equivalence of YIG sphere and fictitious loop antenna. (b) YIG sphere coupling equivalent circuit.

The reciprocity theorem applied to the loop antenna indicates that the voltage at the external terminals XX may be written

$$V = \mu A K \dot{i}_x = \mu K V_s \dot{m}_x. \tag{3}$$

Here, $K = h_x/I$ is a coupling factor relating the small-signal magnetic field at the sphere to the RF current in the uniform transmission line for coaxial and radial lines $K = 1/2\pi r$, where r is the radial distance of the sphere from the line axis. Fig. 3(b) shows the YIG sphere embedded in a coaxial-line lumped model. When Kirchoff's laws are applied to this equivalent circuit, the required coupling state equation, which relates h_x to the uniform-line state variables, is obtained:

$$h_x = \frac{K}{2L_1}(V_1 - V_2 + \mu K V_s(\alpha\gamma H_0 m_x + \gamma H_0 m_z - \alpha\gamma M_0 h_x)). \tag{4}$$

The behavior of the YIG sphere and its coupling to the uniform line are therefore described by the state equations (1), (4).

V. State-Space Analysis of Complete Oscillator Model

The state equations describing the behavior of the constituent parts of the oscillator may be combined to form a matrix equation which applies to the complete oscillator:

$$\{\dot{x}\} = \{A\}\{x\} \tag{5}$$

where $\{x\}$ represents the vector comprising the state variables.

The coefficients of the constant A matrix can be evaluated as previously described from the oscillator physical dimensions, diode dimensions and dc bias current, and the YIG sphere dimensions and applied dc magnetic field. It has been shown [7] that the eigenvalues of the A matrix represent the natural frequencies of the system described by the A matrix. Thus the oscillation frequencies may be determined for a given diode dc bias current and static magnetic field. Hence, the small-signal magnetic tuning curve for the oscillator may be found.

VI. Modified Diode Lumped Model

Fig. 4 compares the computed and measured frequency versus bias-current tuning curves for a simple coaxial IMPATT oscillator (see inset). Curve A refers to the dominant oscillating mode, in which the output power varied linearly with frequency, reaching 120 mW at 40 mA. Curve B represents a subsidiary oscillation with a power output of less than 5 mW. The difference in the computed and measured tuning rates is due to the influence of large-signal effects on the diode reactance. In order to overcome this source of error, the small-signal diode model has been modified to account for the large-signal effects. The modified computed tuning rate agrees well with experiment (Fig. 4).

The diode small-signal avalanche inductance may be written as

$$L_a = \frac{\tau_a}{2\alpha_0' I_0} \tag{6}$$

where τ_a represents the carrier transit time in the avalanche region, α_0' the rate of change of ionization rate with electric field, and I_0 the dc bias current. Scherer [8] has shown that as the RF voltage in-

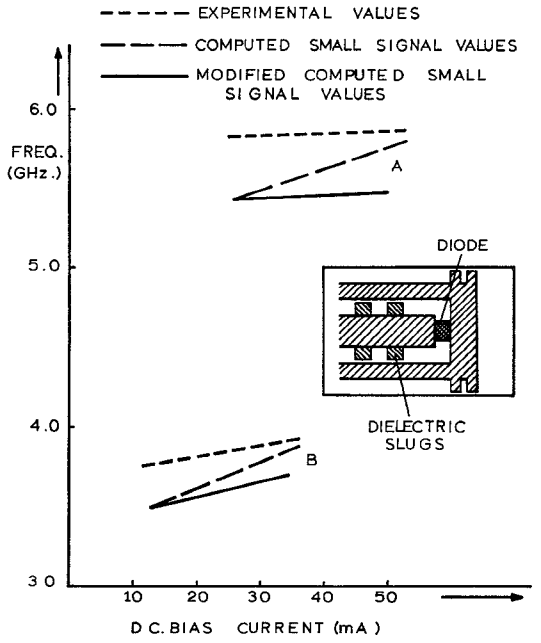

Fig. 4. Experimental and computed tuning curves for dielectric slug coaxial oscillator.

creases for a given I_0, L_a increases. This causes a decrease in oscillator frequency which offsets the increase due to an increase in I_0. This effect may be approximately accounted for by replacing α_0' by a field-dependent value

$$\alpha' = \frac{\alpha_0'}{(1+K_1)^2}. \tag{7}$$

For the oscillator under consideration the output power was found experimentally to vary linearly with dc bias current. By assuming that the diode output power saturates at 500 mW with 100-mA dc bias current, $K_1 = (E_{ac}/E_{dc})$ was found to be given by $K_1^2 = 2.5(I_0 - I_T)$, where I_T is the critical bias current for the occurrence of output power. Hence, for a given dc bias current I_0, the small-signal diode impedance is modified by the insertion of the relevant α' into the A-matrix determination.

VII. Coaxial and Radial Oscillator Magnetic Tuning

The IMPATT diode was a Hewlett-Packard 5082-0400 type with a rated output power of 500 mW at 100-mA dc bias current. From capacitance measurements the following parameters were derived for the diode and used to estimate the A-matrix coefficients:

depletion region width	3.9×10^{-4} cm;
depletion region doping density	0.7×10^{16} cm^{-3};
diode cross-sectional area	1.7×10^{-4} cm^2.

The YIG sphere had a diameter of 0.06 in and a nominal line width of 0.5 Oe.

The coaxial oscillator is shown in Fig. 5 (inset). The computed and measured tuning curves are compared in Fig. 5. Note that at sphere resonance in this tuning mode, the oscillation is quenched, thus limiting the usable tuning range to 220 MHz. The output power varied from 120 mW at low dc magnetic fields to zero at sphere resonance. The measured and predicted frequencies agree to within 3 percent. The magnetic-field independent error may be due to inaccuracy in estimating the mount equivalent circuit.

Fig. 6 indicates the form and tuning performance of the radial-cavity oscillator. In this case the maximum practical sweep deviation is limited to 300 MHz by magnetostatic modes caused by the close proximity to the YIG sphere of the cavity walls. The output power again varied from 150 mW at low magnetic fields to 20 mW at sphere resonance. The discrepancy between measured and computed frequencies is less than 2 percent.

VIII. Conclusions

The small-signal diode lumped model, modified to take some account of large-signal effects, in conjunction with state-space descriptions of the YIG sphere and external microwave cavity, has predicted oscillation frequencies for both coaxial and radial cavity IMPATT-diode magnetically tuned oscillators, which agree within 3 percent with experimental values.

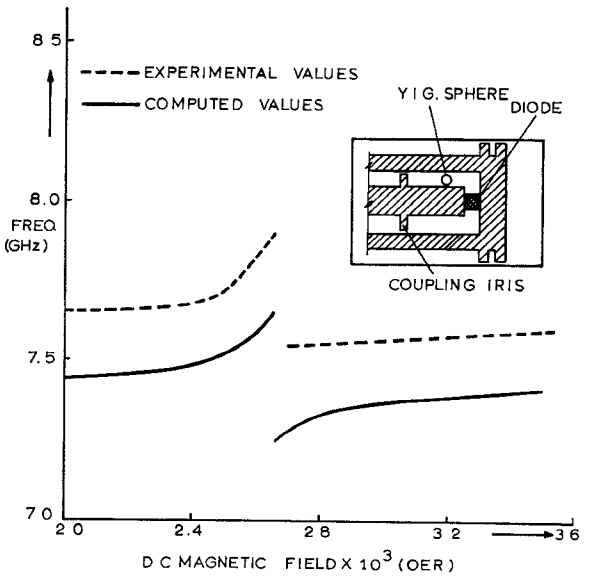

Fig. 5. Experimental and computed tuning curves for magnetically tuned coaxial oscillator.

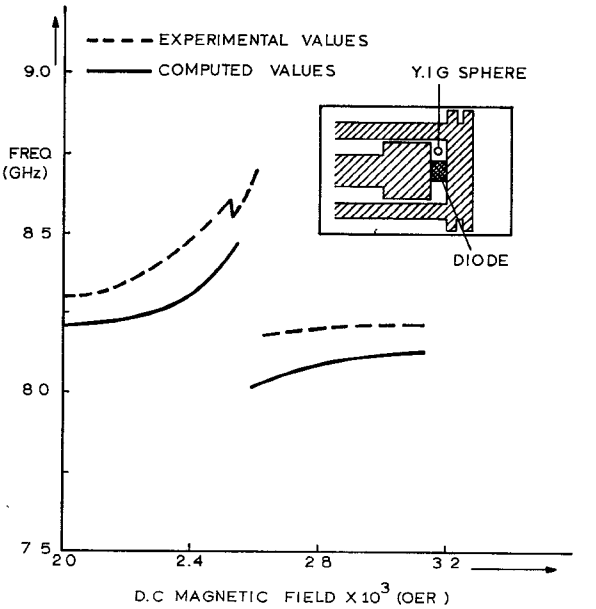

Fig. 6. Experimental and computed tuning curves for magnetically tuned radial-cavity oscillator.

The use of the YIG sphere to perturb the oscillator frequency (rather than to act as the principal external energy-storage mechanism) yields usable frequency deviations of order 300 MHz and output powers which vary with tuning magnetic field.

The segmented buildup of the complete oscillator equivalent circuit, and consequent state-space formulation, enables this analysis method to be applied to oscillators incorporating different cavities, different active devices, and different tuning devices. The method should therefore be of general use in the analysis of active microwave semiconductor device circuits.

References

[1] M. Omori, "Octave electronic tuning of CW Gunn diode using a YIG sphere," *Proc. IEEE* (Corresp.), vol. 57, p. 97, Jan. 1969.
[2] D. C. Hansen, "YIG-tuned transferred electron oscillator using thin film microcircuits," in *IEEE Int. Solid State Circuit Conf. Digest* (Philadelphia, Pa.), pp. 122–123, Feb. 1969.
[3] J. A. C. Stewart, D. R. Conn, and H. R. Mitchell, "State-space analysis of general IMPATT diode small-signal lumped models," *IEEE Trans. Microwave Theory Tech. (Special Issue on Microwave Circuit Aspects of Avalanche-Diode and Transferred Electron Devices)*, vol. MTT-18, pp. 835–842, Nov. 1970.

[4] W. J. Getsinger, "The packaged and mounted diode as a microwave circuit," *IEEE Trans. Microwave Theory Tech.*, vol. MTT-14, pp. 58–69, Feb. 1966.
[5] I. J. H. S. Moore and J. A. C. Stewart, "Analysis of a magnetically tuned coaxial cavity using state-space techniques," *Electron. Lett.*, vol. 6, p. 391, June 1970.
[6] P. S. Carter, G. L. Matthaei, and W. J. Getsinger, "Design criteria for microwave filters and coupling structures," Stanford Res. Inst., Stanford, Calif., Tech. Rep. 8, SRI Project 2326, pp. 8–10, Sept. 1959.
[7] P. H. Roe, *Networks and Systems*. Reading, Mass.: Addison-Wesley, 1966, p. 199.
8] E. F. Scherer, "Large-signal operation of avalanche-diode amplifiers," *IEEE Trans. Microwave Theory Tech. (Special Issue on Microwave Circuit Aspects of Avalanche-Diode and Transferred Electron Devices)*, vol. MTT-18, pp. 922–932, Nov. 1970.

A Magnetically Tunable Microstrip IMPATT Oscillator

B. GLANCE

***Abstract*—Magnetically tunable resonators have been constructed in microstrip on a ferrite substrate. A large tuning range is obtained with an external magnetic field applied in the direction of the RF propagation, 17 MHz/Oe for magnetic fields from 0 to 30 Oe. A variable frequency microstrip oscillator which uses this effect is described; measurements made on an *X*-band IMPATT oscillator illustrate a tuning range from 9.4 to 10.5 GHz with an output power of 330 mW ±0.5 dB.**

I. Introduction

Solid-state microstrip oscillators are nearly fixed frequency sources which can be tuned over only a very limited frequency range by changing the dc current applied to the diode unless the resonant circuit in which they are placed is also tuned in some way. Varactor tuned oscillators [1] provide a solution to this problem but require additional microstrip circuitry and a second power supply for biasing the varator diode. YIG-tuned oscillators [2]–[6] are another solution but need large magnetic fields at microwave frequencies; at *X* band for example a highly homogeneous magnetic field of about 3500 Oe is required in order to avoid spurious modes.

A variable frequency microstrip oscillator with a ferrite substrate is described in this short paper. Such microstrip resonators can be frequency-tuned by a low magnetic field applied in the plane of the ferrite slab. A tuning range of 25 percent has been measured with a magnetic field varying from 0 to about 600 Oe.

II. Propagation in Ferrite-Filled Microstrip Line

Propagation of electromagnetic waves in gyromagnetic media has been the subject of considerable investigation. Most of the analyses have been made for ferrites magnetized at saturation. The propagating mode for wide ferrite-filled microstrip lines is a TEM mode with a scalar permeability. For ferrite substrates which are magnetized at saturation in the direction of propagation, the relative permeability is approximately [7]–[9]

$$\mu_r \approx 1 - \left(\frac{\omega_m}{\omega}\right)^2 - \frac{\omega_0\omega_m}{\omega^2} \qquad (1)$$

with

$$\omega_0 = |\gamma| H_0$$
$$\omega_m = |\gamma| 4\pi M$$

where H_0 is the effective dc magnetic field, $4\pi M_s$ is the saturation magnetization (equal to 2650 G for the ferrite used in this experiment), and $|\gamma|$ is the gyromagnetic constant 2.8 MHz/Oe. The frequency tuning of ferrite-filled microstrip resonators is due to the variation of the permeability with the dc magnetic field. Above saturation the frequency is found to vary about 2 MHz/Oe. This variation is mainly due to the term $\omega_0\omega_m/\omega^2$ of (1). A far more rapid change of frequency with applied magnetic field, about 17 MHz/Oe, has been measured in our experiments for magnetic fields from 0 to about 30 Oe which are far below the saturation field of about 300 Oe. This effect is due to the variation of the permeability from the demagnetized state to the saturated state [10]–[12].

Manuscript received August 16, 1972; revised November 13, 1972.
The author is with Bell Laboratories, Crawford Hill Laboratory, Holmdel, N. J. 07733.

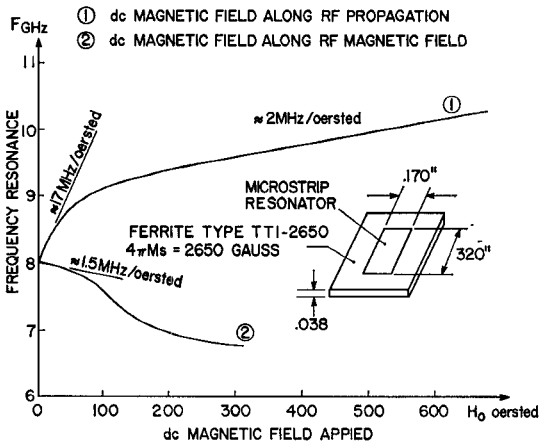

Fig. 1. Resonance frequency of a ferrite-filled microstrip resonator partially magnetized by a variable dc magnetic field directed: ① along the direction of propagation; ② along the direction of the RF magnetic field.

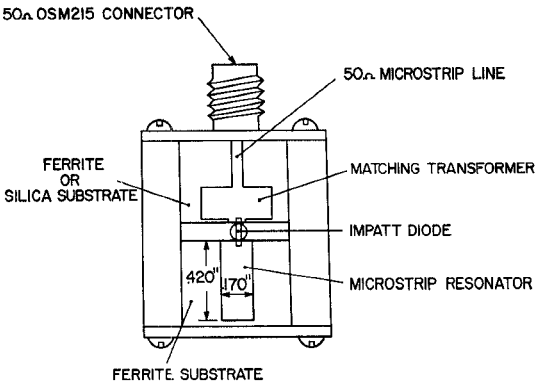

Fig. 2. Schematic drawing of the ferrite-filled microstrip IMPATT oscillator built at *X* band.

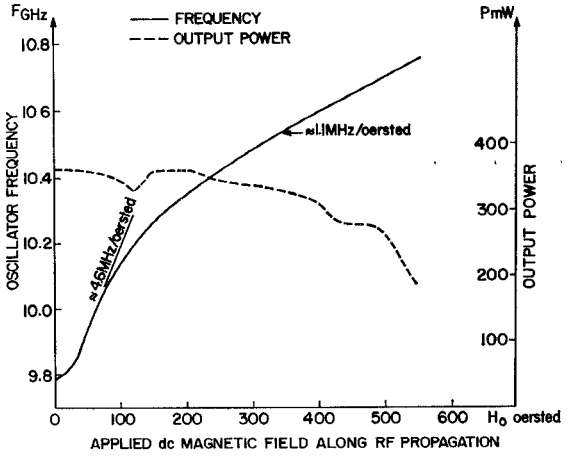

Fig. 3. Power and frequency of the oscillator versus applied dc magnetic field obtained with a microstrip circuit on a ferrite substrate.

Measurements have been made on a ferrite-filled microstrip resonator with the dimensions shown in Fig. 1, which shows also the resonance frequency versus the applied dc magnetic field for: 1) a magnetic field applied along the direction of RF propagation, and 2) a magnetic field applied along the direction of the RF magnetic field.

III. Ferrite-Filled Microstrip Oscillator

As shown in Fig. 2 the microstrip circuit of the oscillator employs two substrates. One substrate is used for the resonator and the other for a matching transformer and output circuit. The diode is mounted between the substrates as shown in Fig. 2.